

Highly Efficient ZVS-ZCS Bidirectional DC-DC Converter for E-Vehicles

B. Sruthi^{1*}, P. Sai Niranjan Kumar²

¹Student, Department of Electrical and Electronics Engineering, G. Narayanamma Institute of Technology and Science, Hyderabad, India

²Assistant Professor, Department of Electrical and Electronics Engineering, G. Narayanamma Institute of Technology and Science, Hyderabad, India

Abstract: In this paper, hybrid energy storage system (ESS), consisting of battery and super capacitor (SC) is used in a standalone photovoltaic system. Since the battery energy storage system is composed by high energy density and low power density and also degradation occurs due to frequent and partial charge/discharge cycles. By integrating super capacitor energy storage system which has high charge/discharge rates, a system having high energy and power capabilities is designed. In this paper non-isolated soft-switching bidirectional DC-DC converter is integrated which is suitable for high step-up and step-down applications. The whole system results in overall life span enhancement of the battery and also reduction in size and cost of the battery. The control scheme is verified using MATLAB/Simulink models.

Keywords: Soft switching, zero voltage switching, zero current switching, Non isolated bidirectional converter.

1. Introduction

The major power conversion devices in an electric vehicle are the charger, inverter and DC-DC converter. For an electric vehicle, some losses are fixed regardless of load, while other losses are linearly and exponentially proportional to the load. Generally, there are three main contributors to losses in a power semiconductor conduction, switching and blocking (or reverse leakage). In some cases, these losses can be ignored but most of the time they tend to sneak up and reduce the efficiency of converter if not properly designed. Sometimes by faster switching in order to minimize losses can lead to problems like over voltage and electromagnetic interference (EMI).

The main aim of this paper is to reduce switching losses by using a non-isolated bidirectional DC-DC converter with interleaved topology. Here MPPT algorithm is used for extraction of maximum power to ensure high efficient operation of PV module. The proposed converter is operated under ZCS and ZVS condition which improves the voltage gain and overall efficiency.

The main objectives of this paper are,

- Reduction in power losses of switches by soft switching.
- Reduction in voltage stress and current stress of the

switches.

- Simulation of proposed system and verification of theoretical analysis.

2. Hybrid Energy Storage System

A standalone PV system containing a battery and super capacitor is used. The PV panel is connected to the load using a non-isolated bidirectional converter and an inverter. The function of the boost converter used at the panel is to extract the maximum power from PV panel using maximum power point tracking (MPPT) algorithm. Hybrid ESS is connected to the load using non isolated bi-directional DC-DC converters. Hybrid ESS is used to maintain the constant DC voltage even if there is a mismatch between generation and demand. When the demand is more than generation, Output voltage drops from its reference value, consequently Hybrid ESS will discharge to provide the surplus demand. Similarly, when the demand is less than the generation, Output voltage increases from its reference value.

Table 1

| Component of system | Specifications |
|---------------------|--|
| PV array | $V_{oc}=37.5V$, $I_{sc}=33.2A$, $P_{mpp}=882.7W$ |
| Battery | Lead acid 24V, 14Ah |
| Super capacitor | 29F, 32V |

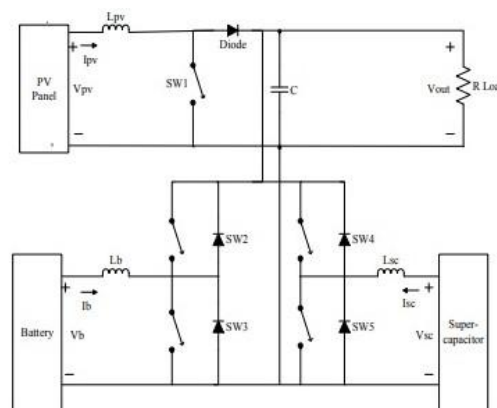


Fig. 1. Photo voltaic system with battery and super capacitor storage system

*Corresponding author: sruthibattina@gmail.com

3. Non Isolated Bidirectional DC-DC Converter

The proposed converter consists of a general buck/boost converter as the main circuit and an auxiliary circuit which includes capacitor C_a , inductor L_a and two high voltage side (HVS) switches S_3 and S_4 .

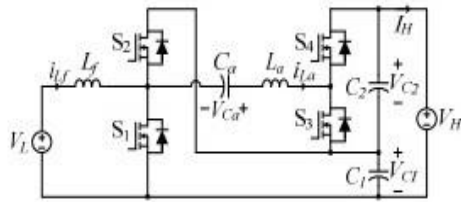


Fig. 2. Bidirectional DC-DC converter

Fig. 3 shows boost mode operation states of the proposed converter.

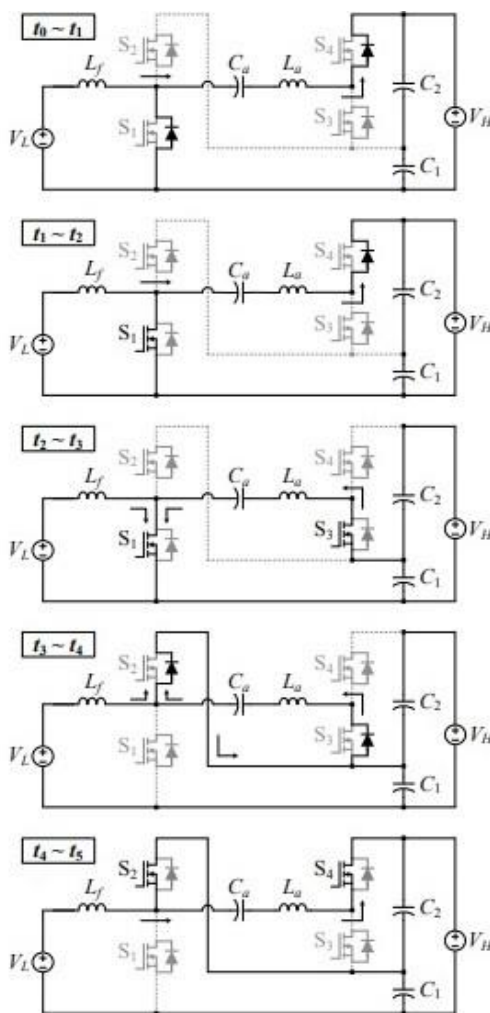


Fig. 3. Boost mode of operation

Boost mode:

Mode 1($t_0 \sim t_1$): Mode begins by turning off of S_2 and S_4 and then the body diodes of S_1 and S_3 are turned on. Gating signal is applied and S_1 is turned on under ZVS condition. I_{L_f} and I_{L_a} starts to increase and decrease respectively.

Mode 2($t_1 \sim t_2$): When I_{L_f} becomes greater than I_{L_a} current

through S_1 is reversed and main channel of S_1 conducts and then I_{L_a} decreases and becomes 0.

Mode 3($t_2 \sim t_3$): I_{L_a} is reversed at t_2 and body diode of S_3 is turned on. Gating signal is applied and S_3 is turned on under ZVS condition, I_{L_a} increases gradually.

Mode 4($t_3 \sim t_4$): S_1 and S_3 are turned off at t_3 and body diodes of S_2 and S_4 are turned on. I_{L_f} and I_{L_a} decreases gradually. S_2 is applied with gating signal and turned on under ZVS condition. As I_{L_a} decreases and becomes 0, S_3 is also turned off under ZCS condition.

Mode 5($t_4 \sim t_5$): Mode starts when I_{L_a} is reversed the body diode of S_4 is turned on under ZVS condition and I_{L_a} increases accordingly.

The waveforms associated with boost mode are shown in Fig. 4.

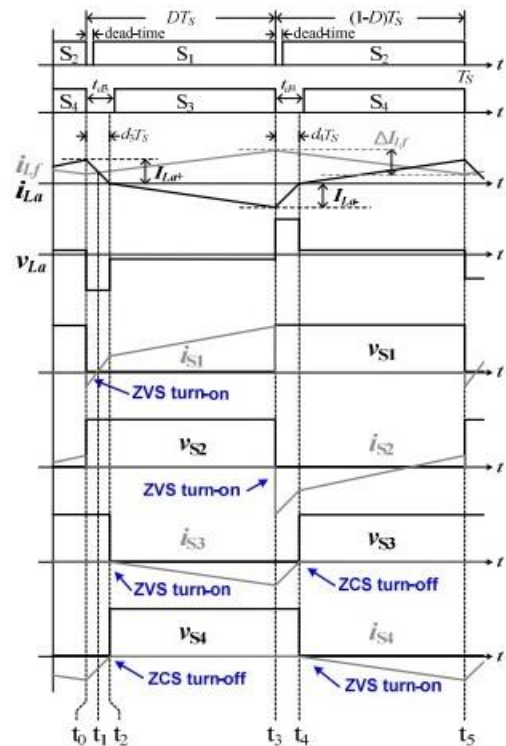


Fig. 4. Waveforms during boost mode of operation

Fig. 5 shows buck mode operation states of the proposed converter. This is the end of one complete cycle.

Buck mode:

Mode 1($t_0 \sim t_1$): Mode begins with turning off of S_2 and S_4 , body diodes of S_1 and S_3 are turned on after parasitic capacitors of S_1 and S_3 are discharged completely. I_{L_f} starts to decrease gradually.

Mode 2($t_1 \sim t_2$): I_{L_a} starts to decrease from t_2 then S_2 and S_3 are turned on. Gating signal of S_3 is applied before reversal of I_{L_a} for ZVS turn on. When I_{L_a} decreases and reaches 0 mode 2 ends.

Mode 3($t_2 \sim t_3$): At t_2 I_{L_a} is reversed and starts to increase with positive peak

Mode 4($t_3 \sim t_4$): S_1 and S_3 are turned off at t_3 and body diodes of S_2 and S_4 are turned on I_{L_a} starts to decrease. Gating

signal is applied to S4 and turned on under ZVS condition. Mode 4 ends when I_{La} becomes 0.

Mode 5 ($t_4 \sim t_5$): When I_{La} becomes greater than I_{Lf} body diode of S1 is turned off under ZCS condition. Parasitic capacitors of S1 is charged and S2 is discharged respectively. Body diode of S2 is turned on and I_{La} decreases and I_{Lf} increases respectively. S2 is turned on using gating signal before I_{La} becomes lesser than I_{Lf} for ZVS turn on.

Mode 6 ($t_5 \sim t_6$): At t_5 current through S2 is reversed, I_{La} decreases and I_{Lf} increases. By the end of mode 6 S2 and S4 are turned off

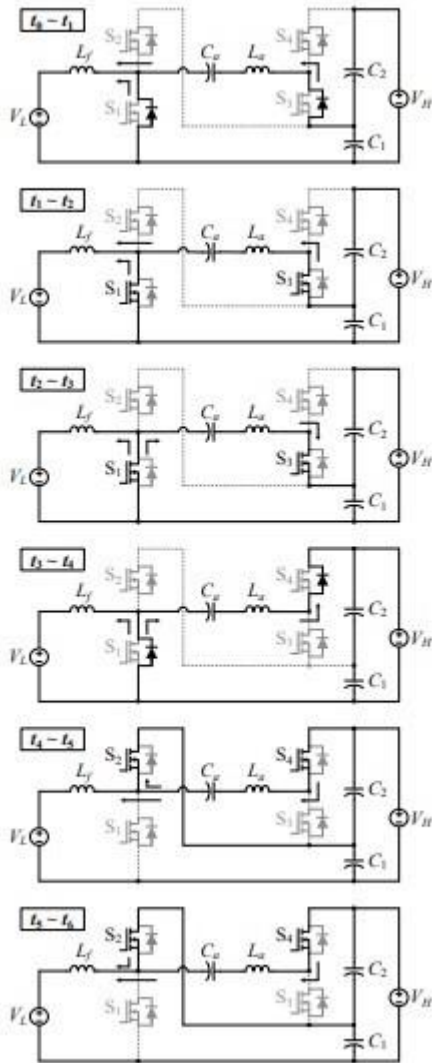


Fig. 5. Buck mode of operation

The waveforms associated with buck mode are shown in fig. 6.

Design specifications:

$$L_f = \frac{V_p D(1-D)}{f_s \Delta I} = \frac{32 \cdot 0.609 \cdot 0.309}{16 \cdot 1000 \cdot 0.3} = 0.355 \text{mH}$$

$$L_{pv} = \frac{V_{in} - \min \times D_{max}}{f_s \Delta I_{(p-p)}} = \frac{0.26 \cdot 17}{5 \cdot 1000 \cdot 6.25} = 0.352 \text{mH}$$

$$L_r = L_a = \frac{1}{2} \frac{V_{in} D}{f_s \Delta I_{in}} = \frac{0.609 \cdot 32}{2 \cdot 16000 \cdot 0.406} = 1.5 \text{mH}$$

$$C_d = I_o \frac{dt}{dV} = \frac{14 \cdot 0.26}{16000 \cdot 0.75} = 300 \mu\text{F}$$

From above equations $C_r = C_{OS,U}$ is less than $30 \mu\text{F}$

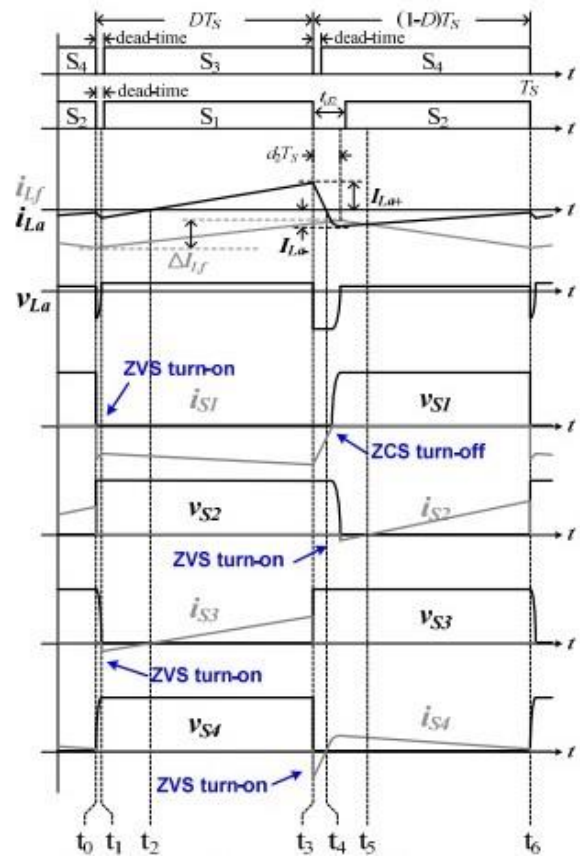


Fig. 6. Waveforms during buck mode of operation

This is the end of one complete cycle.

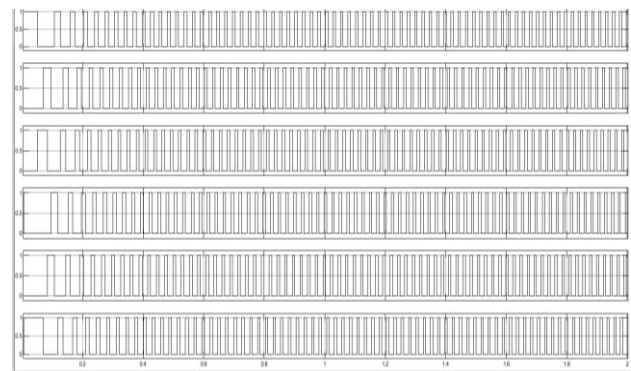


Fig. 7. Gate signals to inverter

4. Results

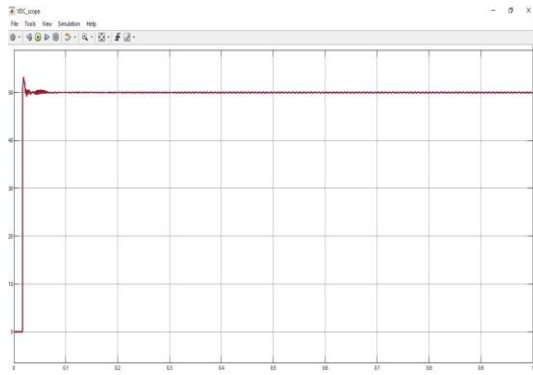


Fig. 8. Output voltage wave form of hard switching

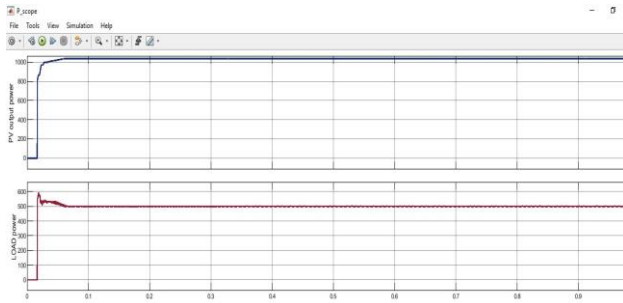


Fig. 9. Output power wave form of hard switching

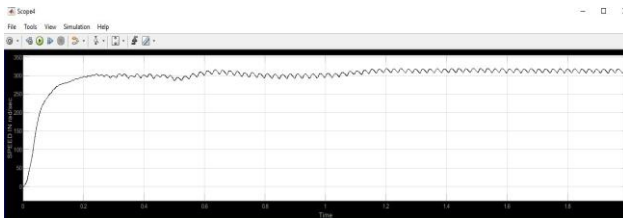


Fig. 10. PMSM load speed wave form in rad/sec (hard switching)



Fig. 11. Output voltage wave form of soft switching

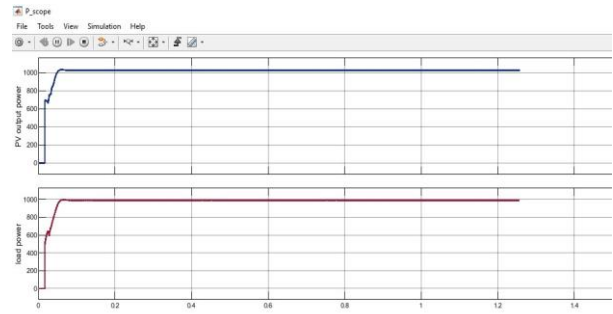


Fig. 12. Output power wave form of soft switching



Fig. 13. PMSM load speed wave form in rad/sec (soft switching)

Table 2

| Gain | Hard Switching | Soft Switching |
|--------------|--|---|
| Voltage gain | $\frac{V_o}{V_{in}} = \frac{50}{37} = 1.35$ | $\frac{V_o}{V_{in}} = \frac{70}{37} = 1.89$ |
| Power gain | $\frac{P_o}{P_{in}} = \frac{500}{1020} = 0.49$ | $\frac{P_o}{P_{in}} = \frac{1000}{1020} = 0.98$ |

5. Conclusion

The proposed converter can achieve ZVS turn on of all switches and ZCS turn of some switches in both boost and buck operations. An optimized switching sequence is presented along with an intermediate switching pattern. The interleaving technique can be applied to reduce the size of passive components and current stresses and improve the overall efficiency of buck boost converter.

References

- [1] M. Kwon, S. Oh and S. Choi, "High Gain Soft-Switching Bidirectional DC-DC Converter for Eco-Friendly Vehicles," in IEEE Transactions on Power Electronics, vol. 29, no. 4, pp. 1659-1666, April 2014.
- [2] L. Yang and T. Liang, "Analysis and Implementation of a Novel Bidirectional DC-DC Converter," in IEEE Transactions on Industrial Electronics, vol. 59, no. 1, pp. 422-434, Jan. 2012.
- [3] F. H. Khan, L. M. Tolbert and W. E. Webb, "Hybrid Electric Vehicle Power Management Solutions Based on Isolated and Nonisolated Configurations of Multilevel Modular Capacitor-Clamped Converter," in IEEE Transactions on Industrial Electronics, vol. 56, no. 8, pp. 3079-3095, Aug. 2009.
- [4] P. Das, S. A. Mousavi and G. Moschopoulos, "Analysis and Design of a Nonisolated Bidirectional ZVS-PWM DC-DC Converter with Coupled Inductors," in IEEE Transactions on Power Electronics, vol. 25, no. 10, pp. 2630-2641, Oct. 2010.
- [5] S. Park, Y. Park, S. Choi, W. Choi and K. Lee, "Soft-Switched Interleaved Boost Converters for High Step-Up and High-Power Applications," in IEEE Transactions on Power Electronics, vol. 26, no. 10, pp. 2906-2914, Oct. 2011.
- [6] S. Park and S. Choi, "Soft-Switched CCM Boost Converters with High Voltage Gain for High-Power Applications," in IEEE Transactions on Power Electronics, vol. 25, no. 5, pp. 1211-1217, May 2010.